Available online at www.sciencedirect.com
ScienceDirect
Engineering Structures 29 (2007) 1569–1579
ENGINEERING STRUCTURES
www.elsevier.com/locate/engstruct

Damage evaluation of three masonry towers by acoustic emission

A. Carpinteri*, G. Lacidogna

Department of Structural Engineering and Geotechnics, Politecnico di Torino, 10129 Turin, Italy

Received 21 July 2005; received in revised form 8 May 2006; accepted 7 August 2006
Available online 23 October 2006

Abstract

This study concerns the structural stability of three medieval towers, "Torre Sineo", "Torre Astesiano" and "Torre Bonino", rising in the centre of Alba, a characteristic town in Piedmont (Italy). The geometrical and structural aspects of the towers were analysed and nondestructive tests were performed to assess the evolution of damage phenomena. The damage processes underway in some portions of the masonry were monitored using the Acoustic Emission (AE) technique. This method makes it possible to estimate the amount of energy released during the fracture process and to obtain information on the criticality of ongoing processes. Finally, an *ad hoc* theory based on fractal concepts for assessing the stability of masonry structures from the data obtained with the AE technique is proposed.

Keywords: Historical towers; Acoustic emission monitoring; Nondestructive technique; Damage assessment; Fractal analysis; Structural stability

1. Introduction

Nondestructive and instrumental investigation methods are currently employed to measure and check the evolution of adverse structural phenomena, such as damage and cracking, and to predict their subsequent developments. The choice of a technique for controlling and monitoring reinforced concrete and masonry structures is strictly correlated to the kind of structure to be analysed and the data to be extracted. In particular, damage assessment for historical masonry buildings is often a complex task [1,2]. It is essential to distinguish between stable damage patterns and damage evolution leading to a catastrophic structural collapse. Some damage patterns can be activated by unpredictable events such as earthquakes, or by inappropriate functional extensions and restorations. In addition, the limited ductility of the masonry, combined with the size of these buildings, results in a rather brittle structural behaviour [3]. This study addresses some of the aforementioned problems deemed of special significance.

Tower geometry was determined through the customary survey methods. Damage, cracking and the evolution of these phenomena over time were assessed through nondestructive techniques: tests with flat-jacks were conducted in order to evaluate the range of stresses affecting the structures; at the same time, the cracking processes taking place in some portions of the masonry structures were monitored using the Acoustic Emission (AE) technique [4]. With this approach it becomes possible to introduce a useful energetic damage parameter for structural assessment based on a correlation between AE activity in a structure and the corresponding activity recorded on masonry elements of different sizes, tested to failure by means of double flat-jacks [5].

2. Description of the three towers

These masonry buildings from the 13th century are the tallest and mightiest medieval towers preserved in Alba (Fig. 1). Torre Sineo is square, 39 m high, and leans to a side by about 1% (Fig. 2). Wall thickness ranges from 2 m at the foundation level to 0.8 m at the top. The bearing walls are *a sacco*, i.e., consist of brick faces enclosing a mixture of rubble and bricks bonded with lime and mortar. Over a height of 15 m, the tower is incorporated in a later building.

Torre Astesiano (Fig. 3) has a similar structure, but has a rectangular base. The filling material is more organised, with brick courses arranged in an almost regular fashion, which, however, are not connected with the outer wall faces. In this case, too, the total thickness of the masonry ranges from 2 m at the bottom to 0.8 m at the top. Total height is about 36 m and

* Corresponding author. Tel.: +39 011 564 4850; fax: +39 011 564 4899.
E-mail address: alberto.carpinteri@polito.it (A. Carpinteri).

0141-0296/$ - see front matter © 2006 Elsevier Ltd. All rights reserved.
doi:10.1016/j.engstruct.2006.08.008

Fig. 1. Overall view of the medieval towers of Alba.

the tower does not lean on any side. It is also incorporated in a later building, approximately 15 m high, built when the tower had been completed.

Torre Bonino (Fig. 4), just under 35 m high, is the least imposing of the towers analysed. The bearing walls are similar to those of Torre Astesiano, save that the lower storeys are coated with a thick layer of plaster of over 10 cm. The thickness of the walls ranges from 1.8 m at the base to 0.6 m at the top. The square shaped structure has been incorporated in a valuable building from the Italian Art Nouveau period.

3. Geometrical survey and cracking network

The geometry of the towers and the buildings they are embedded in was fully acquired and organised within a CAD system. The positions of the openings and the variations in the thickness of the tower walls were carefully recorded, together with the positions of the main cracks observed in the structures. The deviation from verticality of the Sineo Tower was evaluated with an optical instrument. One side of the tower leans to the north. Maximum eccentricity, of 39 cm to the north and 3 cm to the west, was measured at the top. The cracking pattern and the slant of the tower are schematically summarised in Fig. 2.

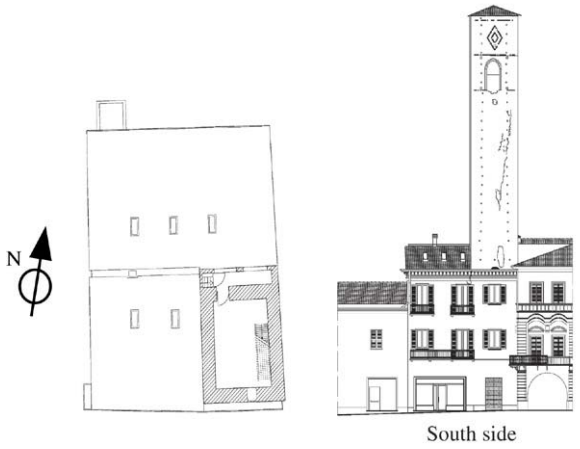

Fig. 3. Torre Astesiano. Plan and elevation view of the tower. Notice the presence of the main crack in the upper part of the tower.

The cracking configuration of the Astesiano Tower is not characterised by cracks distributed over the entire surface of the masonry, but rather by a long vertical crack in the upper part of the southern façade (Fig. 3).

No cracks are visible in the external façades of Torre Bonino (Fig. 4), but the survey revealed the presence of openings and passageways at the different floor levels, linking the tower to the adjacent building. Created during the various restructuring works performed over the years, these openings bring about an appreciable reduction in the bearing capacity of the tower.

4. Flat-jack tests and comparison with similar Italian structures

Tests with single and double flat-jacks were performed on the masonry walls of the towers [5]. These tests were designed to estimate stress values in the masonry at different levels and to assess the elastic modulus and failure strength *in situ*. Table 1 lists the values of mean stresses in the masonry and the Young's modulus as determined with flat-jacks [11] applied to the base of the towers.

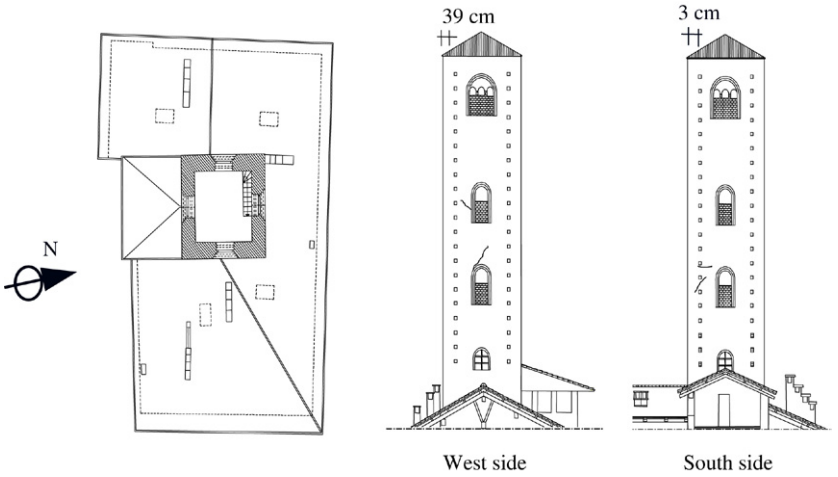

Fig. 2. Torre Sineo. Plan and elevations of two sides of the tower. Notice the presence of cracks near the openings and the deviation from verticality of the tower.

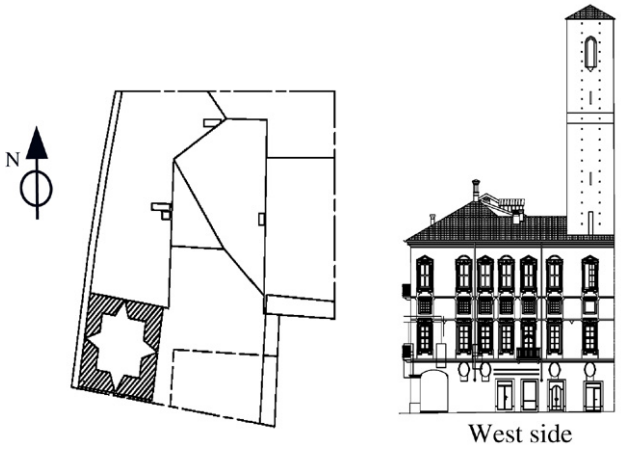

Fig. 4. Torre Bonino. Plan and elevation view of the tower.

Table 1
Results from single and double flat-jack tests

Tower	Compressive stress σ_z (MPa)	Young's modulus E (MPa)
Sineo	0.871	5000
Astesiano	0.480	3300
Bonino	0.592	–

Test results are in substantial agreement with numerical results. They also confirm that the state of stress in these structures is high enough to trigger the opening of cracks in the zones that actually appear damaged [3]. Accordingly, it was decided to compare the static conditions of the Alba towers with those of similar buildings that are part of Italy's historical and architectural heritage. In this manner, test data were compared with those given in an extensive report on ancient Italian masonry towers [6].

In the investigation described in [6], the towers are classified on the basis of their architectural functions, and their different damage levels are identified as a function of cracking configuration. According to the authors, masonry conditions vary from virtually crack-free to badly damaged. In Fig. 5 mean stress values at the base of the towers are correlated to the masonry height/thickness ratio. Despite a certain scatter, the data show a virtually linear correlation. By comparing the values given in [6] with those obtained from the flat-jack tests performed on the Alba towers, it can be seen that, though their slenderness is above average, the towers are characterised by a state of stress that comes close to the average: this can be accounted for by considering that the slabs of the upper storeys of these structures, from the third floor up, are made of thin wooden elements, and this building technique achieves a significant reduction in the dead weight of the structures compared to other towers that are equally slender but have masonry vaults.

5. Detection of damage in the masonry towers

5.1. Acoustic emission equipment and signals analysis

The cracking processes taking place in some portions of the masonry structures were monitored using the AE technique.

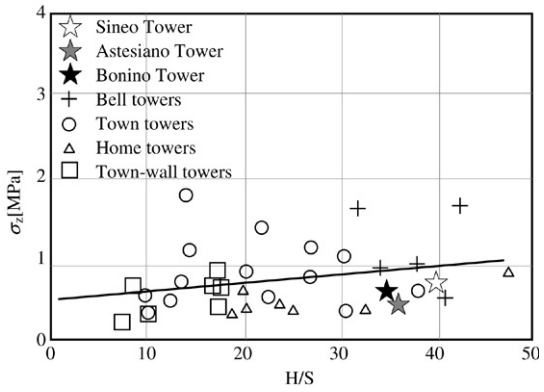

Fig. 5. Vertical stresses at the base of the towers vs. wall height (H) to average wall thickness (S) ratio.

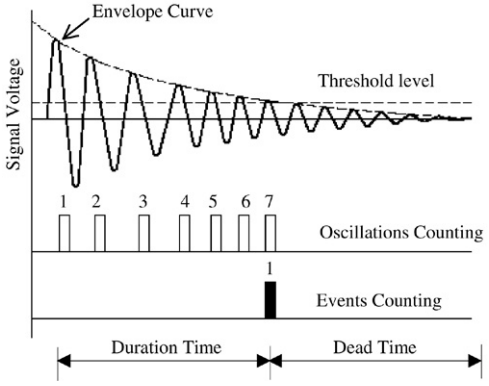

Fig. 6. Signal identified by the transducer and counting methods in the AE technique.

Crack advancement, in fact, is accompanied by the emission of elastic waves which propagate within the bulk of the material (Fig. 6). These waves can be captured and recorded by transducers applied to the surface of the structural elements [4,7,8].

The AE measurement system used by the authors consists of eight piezoelectric (PZT) transducers, calibrated on inclusive frequencies between 50 and 500 kHz, and eight control units. The threshold level for the signals recorded by the equipment, fixed at 100 μV, is amplified up to 100 mV. The system does not provide for the analysis of signal frequency. The amplification gain, given the relationship $\mathrm{dB} = 20 \log_{10} E_u/E_i$, where E_u/E_i is the ratio between the input voltage and the output voltage, turns out to be 60 dB. This is the signal amplification value generally adopted in monitoring AE events in concrete [12,13].

The oscillation counting limit was fixed at 255 oscillations every 120 s [8]. This procedure is referred to as Ring-Down Counting, where the number of counts is proportional to crack advancement. The exponential decay of this signal with respect to time, for a single cracking event, is shown in Fig. 6. The number of counts (N) is obtained by determining the number of times that the signal crosses a certain threshold voltage. The crack growth rate is related to the initial magnitude of the AE elastic wave. However, multiple events which occur simultaneously will also produce a large count. From the

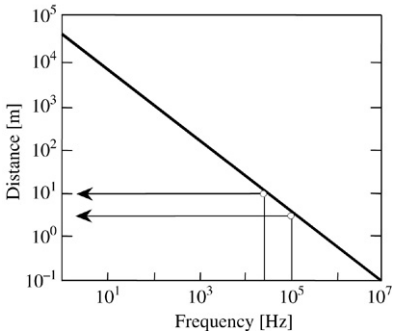

Fig. 7. Acoustic emission relationship between signal detection distance and signal frequency.

literature we know that the duration of a signal emitted during the cracking of a nonmetallic material, such as concrete, is around 2000 μs and that the maximum amplitude of a direct nonamplified signal is greater than 100 μV. Accordingly, since attenuation phenomena can be eliminated by reducing to a few metres the distance of the transducers from the signal generation point, it can be assumed that the system of measurement is able to detect the most meaningful AE events reflecting the evolution of cracking phenomena in the masonry. Attenuation properties, in fact, depend on the frequency range: higher frequency components propagate in masonry with greater attenuation. Based on experimental results (Fig. 7), for a measuring area at a distance of 10 m, only AE waves with frequency components lower than 100 kHz are detectable [12]. In any case, utilising the Ring-Down Counting method, and neglecting the material attenuation properties, the AE counting number (N) can be assumed to be proportional to the quantity of energy released in the masonry volumes during the loading process [14–16].

5.2. Acoustic emission monitoring

For the Sineo Tower, through AE monitoring, two cracks were detected in the inner masonry layer at seventh floor level (Fig. 2). The monitoring process revealed an ongoing damaging process, characterised by slow crack propagation inside the brick walls. In the most damaged zone, crack spreading had come to a halt, the cracks having achieved a new condition of stability, leading towards compressed zones of the masonry. In this particular case it can be seen that, in the zone monitored, each appreciable crack advance is often correlated to a seismic event. In the diagram shown in Fig. 8, the cumulative AE function relating to the area monitored is overlaid with the seismic events recorded in the Alba region during the same time period; the relative intensity of the events is also shown [5,35].

A similar behaviour was observed for Torre Astesiano. This structure was monitored by means of two transducers applied to the inner masonry layer of the tower, at fourth floor level near the tip of the large vertical crack. The results obtained during the monitoring period are summarised in the diagram in Fig. 8. It can be seen how the damage to the masonry and the propagation of the crack, as reflected by the cumulative number of AE counts, evolved progressively over time. A seismic event of magnitude 4.7 on the Richter scale occurred during the monitoring period: from the diagram we can see how the cumulative function of AE counts grew rapidly immediately after the earthquake.

The monitoring of Torre Bonino was performed at first floor level, where the effects of restructuring works have affected the masonry most adversely. Under constant loading, a progressive release of energy is observed, due to a creep phenomenon in the material. A seismic event of magnitude 3 on the Richter scale occurred during the monitoring period (Fig. 8).

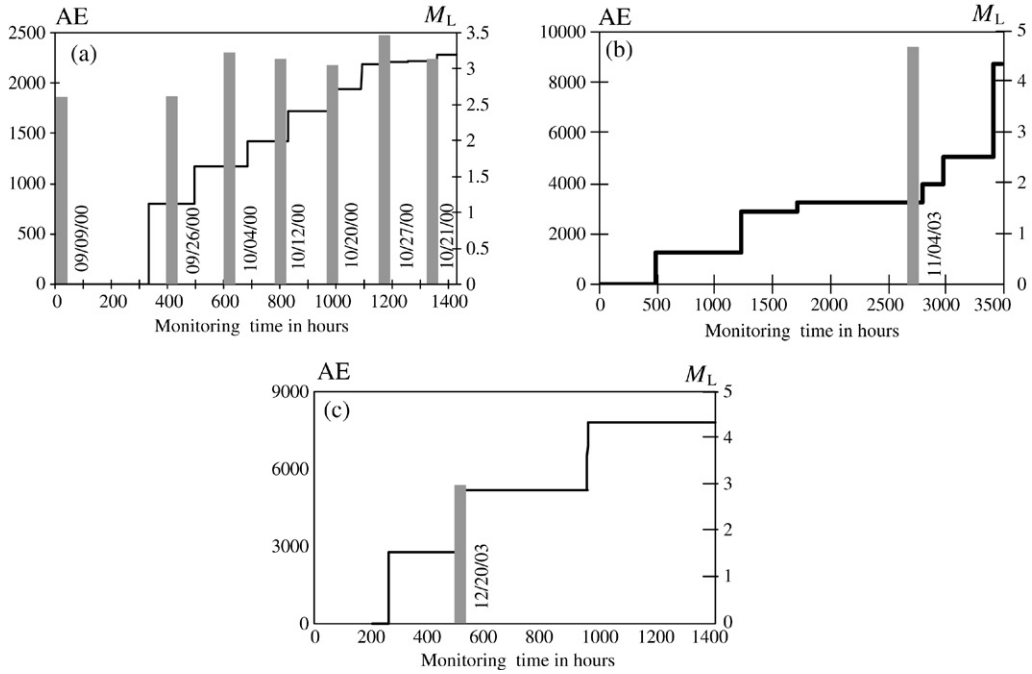

Fig. 8. AE counting number and seismic events in local Richter scale magnitude (M_L). Torre Sineo (a), Torre Astesiano (b), Torre Bonino (c).

During the observation period, the towers behaved as sensitive earthquake receptors. Thus, as can be seen, the AE technique is able to analyse state variations in a certain physical system and can be used as a tool for predicting the occurrence of "catastrophic" events. In many physics problems — e.g., when studying test specimen failure in a laboratory, the modalities of collapse of a civil structure, the natural seismic activity of a volcano or the localisation of the epicentral volume of an earthquake — the zone and the modalities of a collapsed structure are generally analysed "after" the event. This technique can be used instead to identify the premonitory signals that "precede" a catastrophic event, as, in most cases, these warning signs can be captured well in advance [17–20].

6. A fractal criterion for AE monitoring

Fragmentation theories have shown that during microcrack propagation energy dissipation occurs in a fractal domain comprised between a surface and the specimen volume, V [9,10]. On the other hand, during microcrack propagation, acoustic emission counts can be clearly detected. Since the energy dissipated, E, is proportional to the number of AE counts, N, the critical density of acoustic emission counts, Γ_{AE}, can be considered as a size-independent parameter:

$$\Gamma_{\mathrm{AE}} = \frac{N_{\max}}{V^{D/3}}, \tag{1}$$

where Γ_{AE} is the fractal acoustic emission density, and $N_{\max}$ is the total number of counts evaluated at peak-stress, σ_u, i.e., when a critical condition is reached. D is the so-called fractal exponent, comprised between 2 and 3. Eq. (1) predicts a volume-effect on the maximum number of AE counts for a specimen tested to failure, Carpinteri et al. [7,25].

The extent of structural damage can be worked out from the AE data recorded on a reference specimen (subscript r) obtained from the structure and tested to failure. Naturally, the fundamental assumption is that the damage level observed in the reference specimen is proportional to the level reached in the entire structure before monitoring is started.

From Eq. (1) we get

$$N_{\max} = N_{\max r}\left(\frac{V}{V_r}\right)^{D/3}, \tag{2}$$

from which we can obtain the critical number of AE counts, $N_{\max}$, for the structure.

The time dependence of the structural damage observed during the monitoring period, identified by parameter η, can also be correlated to the rate of propagation of the microcracks. If we express the ratio between the cumulative number of AE counts recorded during the monitoring process, N, and the number obtained at the end of the observation period, N_d, as a function of time, t, we get the damage time dependence on AE:

$$\eta = \frac{E}{E_d} = \frac{N}{N_d} = \left(\frac{t}{t_d}\right)^{\beta_t}. \tag{3}$$

In Eq. (3), the values of E_d and N_d do not necessarily correspond to critical conditions ($E_d \leq E_{\max}$; $N_d \leq N_{\max}$) and the t_d parameter must be construed as the time during which the structure has been monitored. By working out the β_t exponent from the data obtained during the observation period, we can make a prediction as to the structure's stability conditions. If $\beta_t < 1$, the damaging process slows down and the structure evolves towards stability conditions, in as much as energy dissipation tends to decrease; if $\beta_t > 1$ the process becomes unstable, and if $\beta_t \cong 1$ the process is metastable, i.e., though it evolves linearly over time, it can reach indifferently either stability or instability conditions [5,35].

7. Overview of the behaviour of masonry under compressive loads

The dependence of masonry properties on the loading system adopted and the geometry of the specimens tested is a significant factor in the determination of the deformation and failure behaviour of masonry under loading. Parametrical analyses of the effects of loading platens on strength characterisation, the amount of energy dissipated and the pre- and post-peak behaviour of masonry specimens are described in but a few theoretical studies [21–23]. However, the problems concerning masonry testing in compression are also encountered when testing other brittle materials such as concrete and rocks, for which more extensive theoretical studies exist, some of them using the acoustic emission technique [24–26].

In the literature, masonry is viewed as a composite and heterogeneous material having inherently variable properties. In particular, in ancient brick masonry structures, such as the Alba towers, this variability is enhanced by natural variations, the manufacturing processes, site conditions and workmanship. In general, the behaviour of a masonry wall or a pier under compression depends on four factors: (i) the characteristic compressive strength of the masonry, (ii) the cross-sectional area resisting the load, (iii) slenderness, (iv) the effective eccentricity of the load at either end and the resulting deflected shape (single or double curvature) [27].

When slenderness effects and the eccentricity of the load are eliminated, the behaviour of masonry under compression is a function of the constituent units of the masonry (the individual bricks) and the mortar. The compressive strength of masonry is usually less than that of the constituent units alone, because of the mortar joints: when masonry is subjected to direct compression and loaded to its full capacity, failure will be initiated by the lateral expansion of the mortar joints (the Poisson's Ratio effect), which causes vertical tensile cracks to form in the masonry units.

7.1. Prism size effects

Prism size effects are another significant aspect characterising the behaviour of masonry under compression. This aspect is also relevant because it is both costly and difficult to test real size structures. The problem of scale effects in masonry under compression has been approached from both the

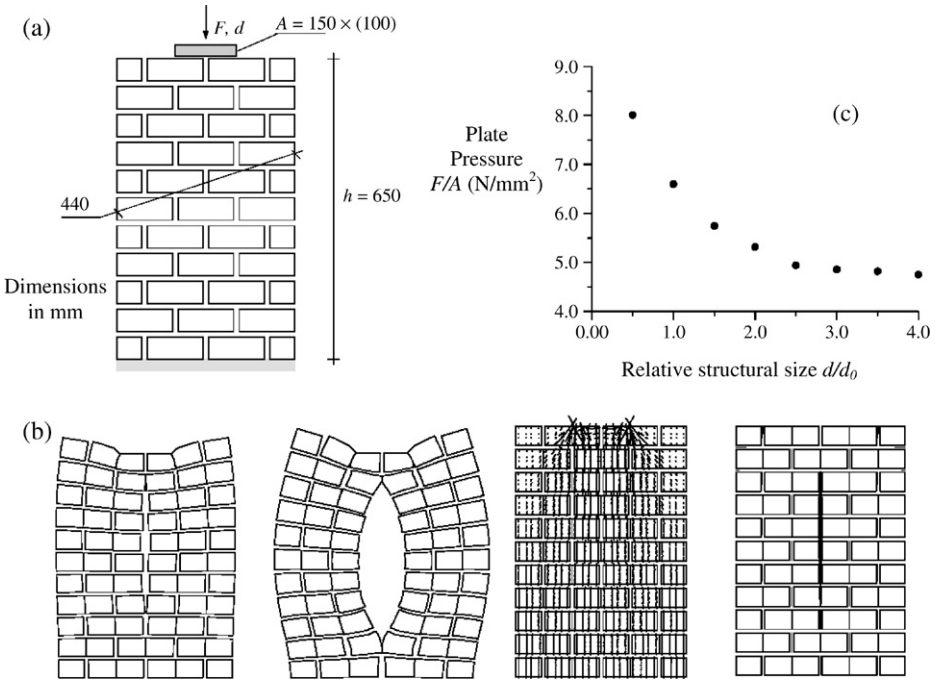

Fig. 9. (a) Masonry pier subjected to point load. The units are $140 \times 50 \times 100$ mm^3 and the joints are 10 mm thick. Nominal pier dimensions, d_0, are given in the figure. (b) Results of the numerical analysis in this order: total deformed mesh at peak load; incremental deformed mesh beyond the peak load; principal stresses; interface relative displacement. (c) Nominal stress versus size in linear scale. (Reprinted from Lourenço [22]).

experimental and the numerical standpoint. Due to the internal structure of masonry, it is possible to discuss two "size-effect" factors: one related to the ratio between nominal dimensions, d, and strength, and the other related to the ratio between unit dimensions and nominal dimensions, d.

Tests performed using units half the real size, Page (1981), one quarter the real size, Gergely et al. (1993), and down to one sixth the real size, Samarasinghe and Hendry (1980), Hughes and Kitching (2000), are not frequent in the literature [28–31]. However, this aspect does not seem to have a decisive influence on the behaviour of the masonry under compression. According to Hughes and Kitching [31], who compared the behaviour of small-scale masonry specimens with the full-scale behaviour of masonry structures constructed with the same constituent units and mortars, an appreciable increase in the compressive strength of the specimens would be observed solely with constituent unit dimensions and mortar joint thickness corresponding to $1/6$ the actual size.

One of the few studies addressing the two aspects from the numerical viewpoint is a report by Lourenço of 1997 [22]. In this report, the author analyses the masonry under construction through a detailed micro-model, in which the constituent units and the mortar are modelled by means of continuum elements, whereas the unit-mortar interface is represented by discontinuous elements. The example given in [22] is an analysis of a masonry pier subject to a point load, Fig. 9. The study of the structural elements is conducted beyond peak load. After peak load, a splitting crack opens in the centre of the pier and propagates in a catastrophic manner. The computed crack path is straight and vertical, indicating that the crack spreads through the pier unit from one end joint to the other. The chosen material parameters represent typical values observed experimentally [32]. The results of the numerical analysis also show that as a function of the scale of the item analysed, i.e., using piers with increasing nominal dimensions, d, the evolution of the cracking configuration remains the same. We always witness the formation of a long vertical crack resulting in the separation of the two piers into two elements whose slenderness is twice that of the original. With increasing specimen scale, instead, we observe an appreciable reduction in failure stresses; see Fig. 9.

In the same study [22], the analysis is repeated with a specimen of the same size, but with an increasing number of units. In this case too, as in [31], the results of the numerical analysis show that with the specimen scale remaining the same, failure stresses in the masonry do not change with varying unit and mortar joint dimensions.

7.2. Prism end-restraint effects

As for the effects of the contact at the bases of the masonry specimens, it has been shown that the behaviour of masonry prisms under uniaxial compressive loading is clearly influenced both by the size of the specimen and by the boundary conditions. Top and bottom bricks remain undamaged when typical steel platens are used, due to the confinement effects produced. On the other hand, when Teflon is placed as an interposition material, the end bricks crack too [23].

Noland and Hanada [21,33] tried to decrease end-restraint effects by lubricating the interface between the prism end and the steel platens of the test machine. This was done by inserting thin Teflon sheets between the smooth gypsum prism cap and the platens. They tested brick masonry prisms with varying h/t (masonry/height thickness ratio) in both

full and reduced end-restraint conditions. Reducing the end-restraint resulted in a tensile splitting failure mode throughout the prism height in prisms of all heights, and a decrease in ultimate strength in otherwise identical end-restrained prisms. The effect of prism height on ultimate strength was not entirely eliminated, however, and led the researchers to conclude that some parameter other than end-restraint was affecting the relationship between prism slenderness and nominal stress. This parameter was the *relative volumes of brick and mortar*. They found that a constant value of "true" compressive strength could be obtained from prisms of varying h/t by introducing a factor based on the relative volumes of the mortar and the bricks.

The test results discussed so far confirm that, during compression tests, though peak stress values are affected by the types of platen used, the trend observed always consists of a reduction in peak stress with increasing specimen slenderness. Similar results are observed in compression tests on concrete specimens [24–26]. However, masonry behaviour differs from that of concrete in that end-restraint effects have marginal consequences on the formation of cracks leading to specimen collapse. Masonry, in fact, is a material made up of different layers of bricks and mortar so that, for slenderness values h/t approximately equal to or higher than 3, platen friction gives rise to the confinement in compression of only the bricks situated at the ends of the specimens.

Moreover, another common element emerges from both experimental and numerical studies: the failure of masonry under compression, whether platens (with or without friction) or point loads applied to the ends are used, is by splitting through the formation of a vertical crack that tends to divide the specimen into elements twice as slender as the original one. This type of failure that occurs after peak load, beyond a certain slenderness ratio, in the softening branch of the stress–strain curve, is hardly affected by the friction generated by the loading platens.

This behaviour, which accounts for the reduction in peak stress with increasing slenderness ratio, can be analysed in numerical terms through a micro-model of the masonry that takes into account the actual heterogeneity of the structural elements and the nonlinear mechanical behaviour of the mortar–masonry interface [34]. Scale effects on the cracking process and the energy dissipated during compression tests, in terms of specimen size and shape, can be clearly identified with the AE technique [35].

7.3. Critical behaviour interpreted by AE

All nondestructive testing (NDT) methods work by introducing some type of energy into the system to be analysed. In AE tests the energy input is the mechanical stresses produced through the application of loads. External forces or internal pressures generate discontinuities or cracks that emit energy waves.

Thus, the AE technique makes it possible to highlight critical phenomena and fracture mechanics scale effects in the masonry by analysing, through a statistical and fractal approach, the microscopic and mesoscopic phenomena interacting, with a view to defining the behaviour of the masonry on a structural scale. This approach does not require a detailed characterisation of the local states of stress and the cracking conditions of the elements monitored, the only element to be determined being the amount of energy that the masonry is able to dissipate up to the onset of the critical conditions which, according to Eq. (1), coincides with the peak stress.

These critical conditions are reached in relation to a certain distribution of the defects, which is deemed independent of the state of stress and crack orientation [20]. Accordingly, the monitoring method proposed, taking its cue from fragmentation theory, is designed to quantify the energy dissipated during the damaging process by the AE counting. The identification of critical conditions is not entrusted to an analysis of the loading process; rather, it depends primarily on the distribution and evolution of crack patterns.

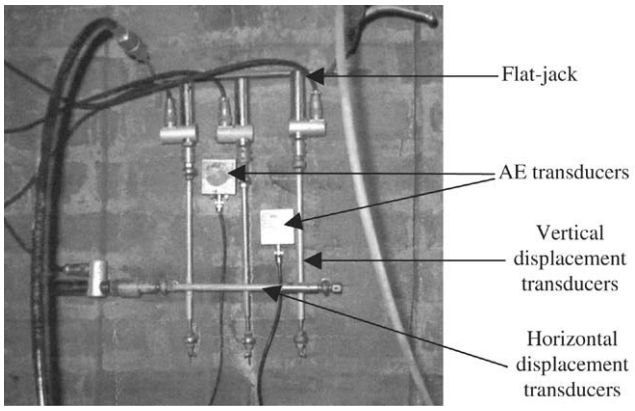

Fig. 10. Combined flat-jack test and AE monitoring.

8. Flat-jack and AE tests

Flat-jack testing is a versatile and powerful technique that provides significant information on the mechanical properties of historical constructions. The first applications of this technique on some historical monuments [36] clearly showed its great potential. The test is only slightly destructive, and this is why it is now widely accepted and used by monument monitoring and rehabilitation experts [37,38]. When double jacks are used, this test works according to the same principle as a standard compressive test. The difference is that it is performed *in situ* and the load is applied by means of two flat-jacks instead of the loading platens. The test method is based on the following assumptions: the masonry surrounding the slot notches is homogenous; the stress applied to the masonry by the flat-jacks is uniform and the state of stress in the test prism is uniaxial.

In order to assess the extent of damage in the zone monitored using the AE technique, a compressive test was conducted on the masonry through the combined use of double jacks and AE sensors (Fig. 10). The tests were carried out with flat-jacks measuring 24×12 cm^2. The cuts made into the masonry wall to obtain a smaller-sized specimen were made into two horizontal mortar joints spaced about 30 cm apart.

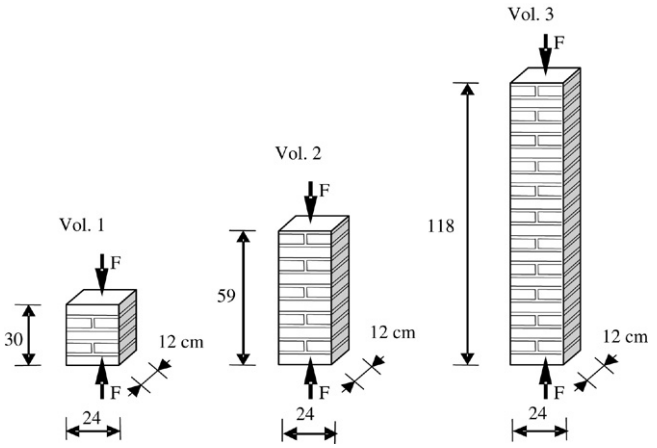

Fig. 11. Masonry elements tested in compression by means of double flat-jacks and AE sensors.

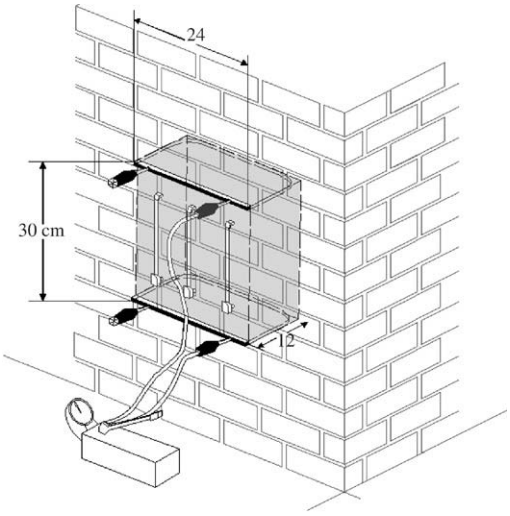

Fig. 12. Typical set-up for *in situ* flat-jack test. The dimensions given are those of the specimen referred to as Vol. 1. (Reprinted from Gregorczyk and Lourenço [38]).

The minimum slenderness ratio of the specimens was $h/t > 2.5$. This made it possible to reduce the friction effects on masonry behaviour arising from the action of the flat-jacks. During the tests, the stress–strain relationship of the masonry was determined by gradually increasing the pressure applied by the flat-jacks in the course of three loading–unloading cycles. Peak compressive strength was obtained from the load–displacement diagram, when the latter became highly nonlinear, denoting imminent failure. For the Astesiano Tower, compressive tests were performed on three different masonry sections at third storey level. The prismatic masonry volumes tested in compression were delimited crosswise by vertical cuts (Fig. 11). A typical setup of a compressive test *in situ* is shown in Fig. 12. The tests were performed in keeping with the procedures specified in ASTM 1991 [11], other than for the vertical cuts produced in order to eliminate, in the cracked element, the influence of the adjacent masonry portions. Fig. 13 shows the results obtained from these tests for the intermediate element (Vol. 2). Similar results were obtained for the other

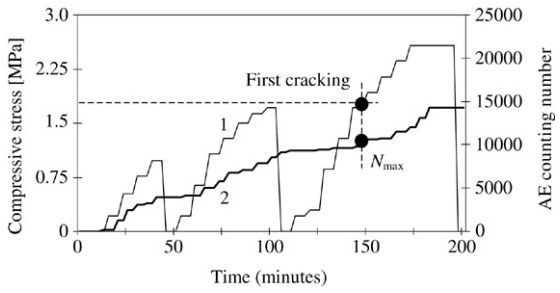

Fig. 13. Double flat-jack test on Vol. 2. Cumulative number of AE counts (2) versus cyclic loading (1).

Table 2
Experimental values obtained from flat-jack tests and AE measurements

Specimen	Volume (cm^3)	Peak stress (MPa)	N_{max} at σ_u
Vol. 1	8640	2.07	~6500
Vol. 2	16 992	1.61	~12 000
Vol. 3	33 984	1.59	~18 000

two elements. The figure also shows the three loading cycles performed as a function of time and the diagram of the cumulative number of AE counts. From the AE diagram it can be clearly seen that the material releases energy when the stress level reached previously is exceeded (*Kaiser effect* [16]). Moreover, from the diagram, we find that the cumulative number of AE counts at failure stress (i.e. before the critical condition is reached) is $N_{max} \cong 12\,000$. The experimental results obtained on the three masonry elements are summarised in Table 2.

8.1. Size effects on AE

As can be seen from Table 2, in compressive tests the peak stress in the masonry specimen is a decreasing function of the slenderness ratio, whereas the cumulative number of AE counts increases with increasing specimen volume. The pre-peak portion of the stress–strain curves shows that specimen slenderness has significant effects on peak stresses σ_u, and size effects are highly significant on the critical number of acoustic emission N_{max}.

From a statistical analysis of the experimental data, parameters D and Γ_{AE} (Eq. (1)) can be quantified [5]. Parameter D represents the slope, in the bilogarithmic diagram, of the curve correlating N_{max} to specimen volume. By best-fitting, we obtain $D/3 \cong 0.743$ (Fig. 14), so that the fractal exponent, as predicted by fragmentation theories, turns out to be between 2 and 3 ($D \cong 2.23$). Moreover, the critical value of fractal AE density turns out to be $\Gamma_{AE} \cong 8.00\ cm^{-2.23}$.

During the compressive tests it was determined that a change in specimen shape had no appreciable effects on the configuration of damage patterns. As pointed out in Section 7, in fact, even the use of flat-jacks invariably determines the formation of a vertical crack plane, which tends to split the specimen into two separate elements. Fractured areas are more deformed, while unfractured portions recover

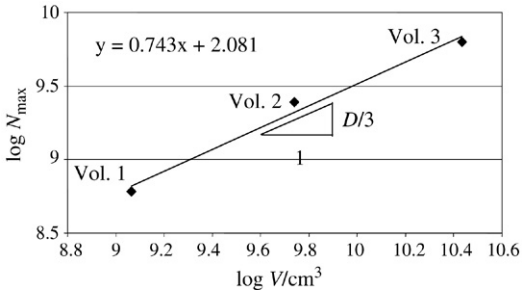

Fig. 14. Volume effect on N_{max}.

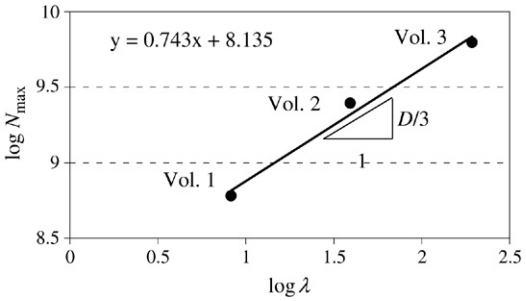

Fig. 15. Shape-effect on N_{max}.

their deformations. When critical conditions are reached, in specimens with greater slenderness the damaged volume is larger but peak stress is lower, compared to lower slenderness specimens. Peak stress, in fact, can be correlated to the quantity of defects present in the materials, whilst damaged volume is proportional to the released energy measured by the AE technique, and hence is proportional to the critical number of acoustic emission N_{max}.

In general, the effects of slenderness on parameter N_{max} is proportional to the area subtended by the stress–strain curve. This area is correlated to the ductility of the material, which, as a rule, is not proportional to its strength. For these reasons, when monitoring full scale structures, it is reasonable to make predictions on the maximum number of AEs that would lead to the critical stage, by taking into account total volume damaged. An example is given in the next section.

On the other hand, the scale effects associated with the critical number of acoustic emission N_{max} would not change even if we wanted to consider the slenderness of the specimens analysed in lieu their volume.

In the bilogarithmic plane, Eq. (1) can be written as

$$\log N_{max} = \log \Gamma_{AE} + \frac{D}{3} \log V, \tag{4}$$

with a slope equal to $D/3$. Considering specimens with base area A (depth b and thickness t) and height h, their volume will be $V = Ah = bth$. Introducing the slenderness $\lambda = h/t$, we get $V = Ah = bt^2\lambda$, and hence Eq. (4) becomes

$$\log N_{max} = \log[\Gamma_{AE}(bt^2)^{D/3}] + \frac{D}{3} \log \lambda, \tag{5}$$

predicting a shape effect on AE. As can be seen from the diagrams in Figs. 14 and 15, slope $D/3$ of the regression line on the bilogarithmic plane does not change, in accordance with Eqs. (4) and (5). Thus, it becomes apparent that from the acoustic emission point of view, the energy released during a compression test essentially depends on the volume of the masonry in compression, even if it is evaluated as a function of specimen slenderness.

9. Damage level in the towers

During the observation period, which lasted 60 days for the Sineo Tower, 146 days for the Astesiano Tower, and 58 days for the Bonino Tower, the number N of AE counts recorded was ≅2250, ≅9000 and ≅ 8000, respectively (Fig. 8). Through earlier tests performed on rubble filled masonry, 80 cm thick, and hence characterised by appreciable discontinuities, it was ascertained that the transducers were able to pick up the AE signals from a distance of up to 10 m from their points of application and to a depth of 12 cm, i.e., over a length corresponding to the thickness of the outer layer of bricks [5].

Since the average width of the sides of the towers is about 500 cm, the total volume monitored by the transducers will be $V \cong 500 \times 2000 \times 12 = 1.2 \times 10^7$ cm^3. From Eq. (1), using fractal exponent $D \cong 2.23$ and the critical value of fractal acoustic emission density, $\Gamma_{AE} \cong 8.00$ cm$^{-2.23}$, we obtain a critical AE number of $N_{max} \cong 1.46 \times 10^6$. Introducing the values of N_{max} into Eq. (3), we get $\eta \cong 0.154\%$ for Torre Sineo, $\eta \cong 0.616\%$ for Torre Astesiano and $\eta \cong 0.550\%$ for Torre Bonino. These values represent, in percentage terms, the amount of energy released with respect to the energy that would cause the ultimate damage of the volumes monitored. Clearly, as previously mentioned in Section 6, the fundamental assumption underlying these predictions is that the damage level observed in the reference specimens before testing is proportional to the level reached in the entire structure before starting monitoring.

Finally, in order to obtain indications on the rate of growth of the damage process in the towers, as given in Eq. (3), the data obtained with the AE technique were subjected to best-fitting in the bilogarithmic plane. This yielded a slant $\beta_t \cong 0.648$ for the Sineo Tower, $\beta_t \cong 1.041$ for the Astesiano Tower and $\beta_t \cong 0.491$ for the Bonino Tower (Fig. 16). These results confirm how the damage process stabilised in the Sineo and Bonino Towers during the monitoring period, whereas for the Astesiano Tower it evolved towards a condition of instability according to a quasi-linear progression over time. In fact, if we introduce the values of N and N_{max} obtained for Torre Astesiano into Eq. (3), with $\beta_t = 1.041$, we get $t/t_{max} \cong 7.532 \times 10^{-3}$. The lifetime of this structure is therefore defined, in terms of time before the maximum number of AE counts is reached in the zone analysed, at about 53 years.

10. Conclusions

Many ancient masonry towers are present in the Italian territory. In some cases these structures are at risk on account of the intensity of the stresses they are subjected to and the nonhomogeneity of the resisting sections. In order to

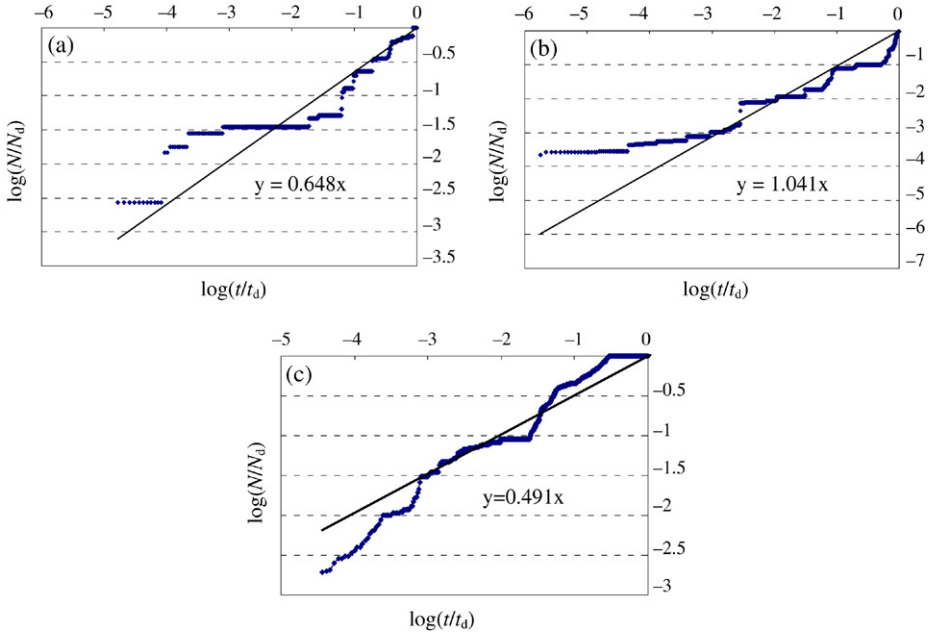

Fig. 16. Evolution of damage: Torre Sineo (a), Torre Astesiano (b), Torre Bonino (c).

preserve this inestimable cultural heritage, a sound safety assessment should take into account the evolution and the interaction of different damage phenomena. In this connection, AE monitoring can be highly effective.

This technique makes it possible to introduce an energy-based damage parameter for structural assessment which establishes a correlation between AE activity in a structure and the corresponding activity recorded on specimens taken from the structure and tested to failure. Moreover, by performing compressive tests through the combined use of double flat-jacks and AE sensors, the safety of structures undergoing damage and degradation processes can be efficiently evaluated *in situ*.

Acknowledgements

This research was carried out with the financial support of the Ministry of University and Scientific Research (MIUR) and of the European Union (EU). The authors would like to thank the City of Alba and Dr. Eng. Massimo Reggio for their indispensable collaboration and Architects Massimo Aprile and Luigi Bacco for the technical support provided in the structural monitoring.

References

[1] Carpinteri A, Bocca P, editors. Damage and diagnosis of materials and structures. In: Proc. of DDMS 91. 1991.

[2] Anzani A, Binda L, Mirabella Roberti G. The effect of heavy persistent actions into the behaviour of ancient masonry. Materials and Structures 2000;33:251–61.

[3] Carpinteri A, Invernizzi S, Lacidogna G. In situ damage assessment and nonlinear modeling of an historical masonry tower. Engineering Structures 2005;27:387–95.

[4] Carpinteri A, Lacidogna G, Pugno N. A fractal approach for damage detection in concrete and masonry structures by the acoustic emission technique. Acoustique et Techniques 2004;38:31–7.

[5] Carpinteri A, Lacidogna G. Structural integrity assessment of medieval towers. In: Modena C, Lourenço PB, Roca P, editors. Proc. of the 4th int. seminar on structural analysis of historical constructions, vol. 1. 2004. p. 523–32.

[6] Binda L, Bertocchi E, Trussardi D. Torri in muratura. Una metodologia per la valutazione della sicurezza. Recupero e Conservazione 1997;18: 26–34 [in Italian].

[7] Carpinteri A, Lacidogna G, Pugno N. Damage diagnosis and life-time assessment of concrete and masonry structures by an acoustic emission technique. In: Li VC, Leung CKY, Willam KJ, Billington SL, editors. Proc. of the 5th int. conf. on fracture mechanics of concrete and concrete structures, vol. 1. 2004. p. 31–40.

[8] Carpinteri A, Lacidogna G. Damage monitoring of an historical masonry building by the acoustic emission technique. Materials and Structures 2006;39:143–9.

[9] Carpinteri A, Pugno N. Fractal fragmentation theory for shape effects of quasi-brittle materials in compression. Magazine of Concrete Research 2002;54:473–80.

[10] Carpinteri A, Lacidogna G, Pugno N. Scaling of energy dissipation in crushing and fragmentation: A fractal and statistical analysis based on particle size distribution. International Journal of Fracture 2004;129: 131–9.

[11] ASTM. Standard test method for in situ compressive stress within solid unit masonry estimated using flat-jack measurements. ASTM C1196-91. Philadelphia; 1991.

[12] Ohtsu M. The history and development of acoustic emission in concrete engineering. Magazine of Concrete Research 1996;48:321–30.

[13] Shah P, Li Z. Localization of microcracking in concrete under uniaxial tension. ACI Materials Journal 1994;91:372–81.

[14] Pollock AA. Acoustic emission-2: Acoustic emission amplitudes. Non-Destructive Testing 1973;6:264–9.

[15] Brindley BJ, Holt J, Palmer IG. Acoustic emission-3: The use of ring-down counting. Non-Destructive Testing 1973;6:299–306.

[16] Kaiser J. An investigation into the occurrence of noises in tensile tests, or a study of acoustic phenomena in tensile tests. Ph. D. dissertation. Munich (FRG): Technische Hochschule München; 1950.

[17] Zapperi S, Vespignani A, Stanley HE. Plasticity and avalanche behaviour in microfracturing phenomena. Nature 1997;388:658–60.

[18] Kapiris P, Balasis G, Kopanas J, Antonopoulos G, Peratzakis A, Eftaxias K. Scaling similarities of multiple fracturing of solid materials. Nonlinear Processes in Geophysics 2004;11:137–51.

[19] Rundle JB, Turcotte DL, Shcherbakov R, Klein W, Sammis C. Statistical physics approach to understanding the multiscale dynamics of earthquake fault systems. Reviews of Geophysics 2003;41:1–30.
[20] Shcherbakov R, Turcotte DL. Damage and self-similarity in fracture. Theoretical and Applied Fracture Mechanics 2003;39:245–58.
[21] Kingsley GR, Noland JL, Schuller MP. The effect of slenderness and end restraint on the behavior of masonry prisms — A literature review. TMS Journal 1992;10:31–47.
[22] Lourenço PB. Two aspects related to the analysis of masonry structures: Size effect and parameter sensitivity. TNO Building and Construction Research, Computational Mechanics, TNO-BOUW report no. 97-NM-R1533. 1997.
[23] Vermeltfoort AT. Brick-mortar interaction in masonry under compression. In: University Press Facilities. Eindhoven (The Netherlands): Eindhoven University of Technology; 2005.
[24] Carpinteri A. Scaling laws and renormalization groups for strength and toughness of disordered materials. International Journal of Solids and Structures 1994;31:291–302.
[25] Carpinteri A, Lacidogna G, Pugno N. Structural damage diagnosis and life-time assessment by acoustic emission monitoring. Engineering Fracture Mechanics 2007;74:273–89. doi:10.1016/j.engfracmech.2006.01.036.
[26] Carpinteri A, Ferro G, Monetto I. Scale effects in uniaxially compressed concrete specimens. Magazine of Concrete Research 1999;51:217–25.
[27] Lawrence S, Page A. Design of clay masonry for compression — Manual 6. Baulkham Hills BC (Australia): Clay Brick and Paver Institute (CBPI); 2004. p. 1–48.
[28] Page AW. The biaxial compressive strength of brick masonry. Proceedings of The Institution Civil Engineers 1981;71(2):893–906.
[29] Gergely P, White RN, Zawilinski D, Mosalam K. The interaction of masonry in-fill and steel or concrete frames. In: Proc. 1993 nat. earthquake conf. 1993; 2: 183–91.
[30] Samarasinghe W, Hendry AW. The strength of brickwork under biaxial tensile and compressive stress. In: Proc. 7th int. symp. on load bearing brickwork. 1980. p. 129–40.
[31] Hughes TG, Kitching N. Small scale testing of masonry. In: Proc. 12th int. brick/block masonry conf. 2000. p. 25–28.
[32] Lourenço PB. Computational strategies for masonry structures. Dissertation. Delft (The Netherlands): Delft University of Technology; 1996.
[33] Noland JL, Hanada KT, Feng CC. The effect of slenderness and end conditions on the strength of clay unit prisms. In: Proc. of the first North American masonry conf. 1978.
[34] Lourenço PB, Rots JG, Blaauwendraad J. Two approaches for the analysis of masonry structures: Micro and macro-modeling. HERON 1995;40: 313–40.
[35] Carpinteri A, Lacidogna G. Structural monitoring and integrity assessment of medieval towers. ASCE Journal of Structural Engineering 2006;132(11) [in press].
[36] Rossi PP. Analysis of mechanical characteristics of brick masonry tested by means of in situ tests. In: 6th Int. brick/block masonry conf. 1982.
[37] Binda L, Tiraboschi C. Flat-jack test as a slightly destructive technique for the diagnosis of brick and stone masonry structures. International Journal for Restoration of Buildings and Monuments 1999;449–72.
[38] Gregorczyk P, Lourenço PB. A review on flat-jack testing. Engenharia Civil UM 2000;9:39–50.